Electronic Supplementary Information

Extremely low self-discharge solid-state supercapacitor via confinement effect of ion transfer

Zixing Wang[a], Xiang Chu[a], Zhong Xu[a], Hai Su[c], Cheng Yan[a], Fangyan Liu[a], Bingni Gu[a], Haichao Huang[a], Da Xiong[a], Hepeng Zhang[a], Weili Deng[a], Haitao Zhang[*, a], Weiqing Yang[*, a,b]

[a] Key Laboratory of Advanced Technologies of Materials (Ministry of Education), School of Materials Science and Engineering, Southwest Jiaotong University, Chengdu 610031, PR China

[b] State Key Laboratory of Traction Power, Southwest Jiaotong University, Chengdu 610031, PR China

[c] School of Materials Science and Engineering, Key Laboratory of Advanced Ceramics and Machining Technology (Ministry of Education), Tianjin Key Laboratory of Composite and Functional Materials and Tianjin Key Laboratory of Molecular Optoelectronic Science, Tianjin University, Tianjin 300072, PR China

[*] Correspondence should be addressed to W. Yang (e-mail: wqyang@swjtu.edu.cn) or H. Zhang (e-mail: haitaozhang@swjtu.edu.cn).

Supplementary Figures

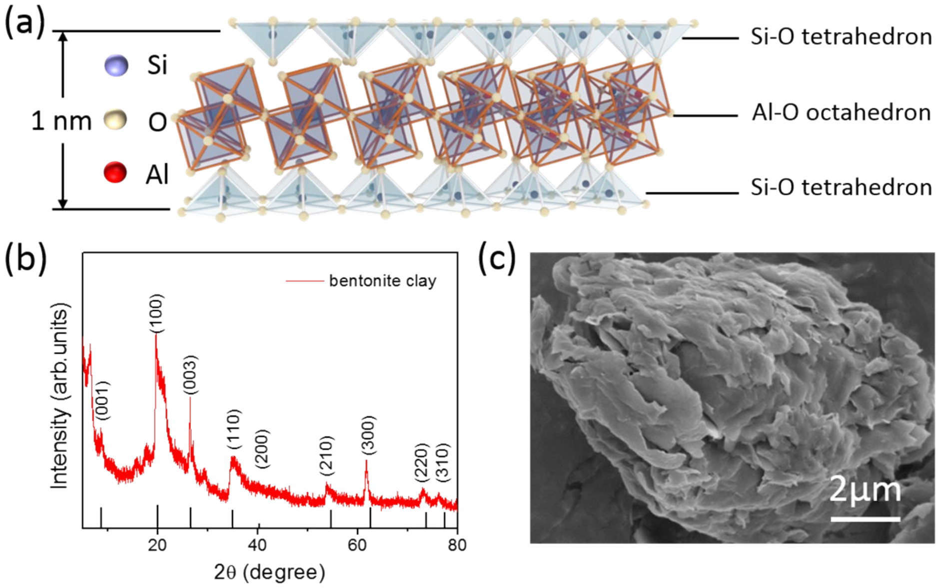

Fig. S1 The layered structure of bentonite clay. (a) Schematic illustration of the crystal structure of the bentonite clay. **(b)** The XRD patterns of the bentonite clay. **(c)** SEM image of the bentonite clay. The lattice structure of bentonite clay consists of ~1 nm thin layers with an octahedral layer of Al-O unit sandwiched between two tetrahedral layers of Si-O units.

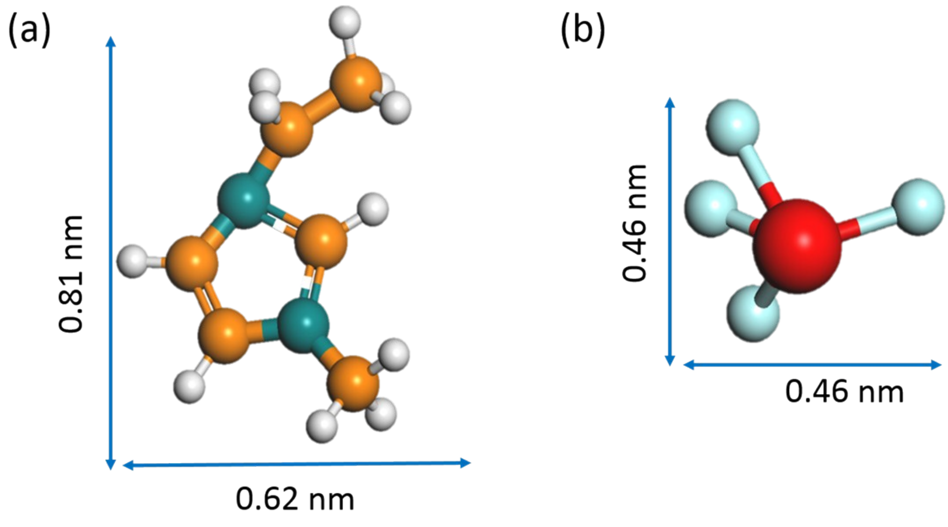

Fig. S2 Ion models for a) $EMIM^+$ and b) $BF4^-$.

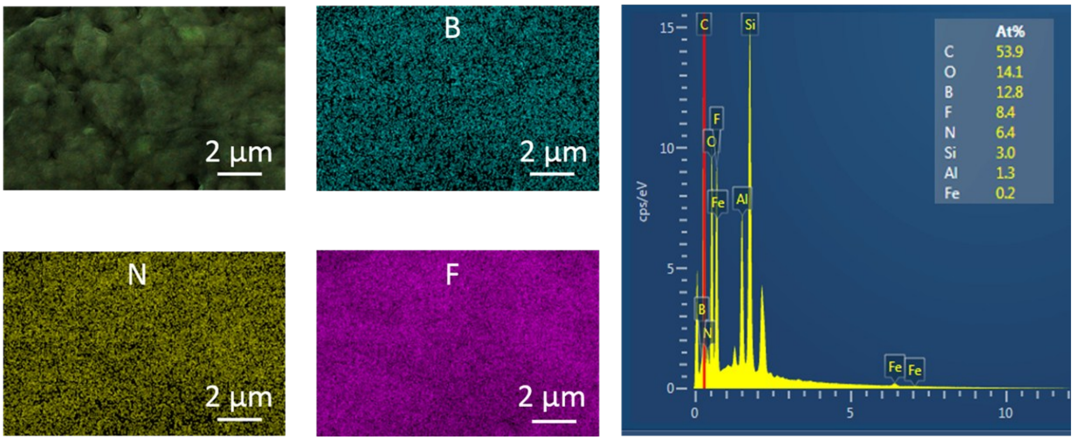

Fig. S3 EDS images of the bentonite after self-discharge process.

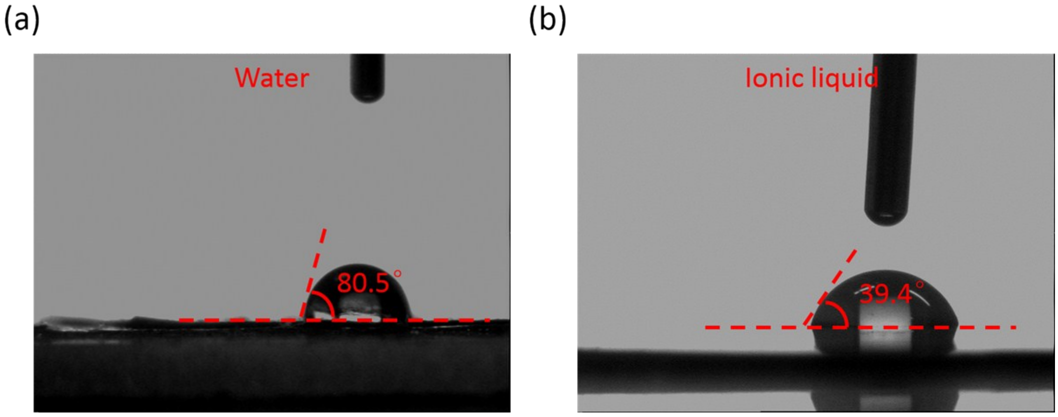

Fig. S4 The Contact Angle test of the solid film produced. (a) Water and (b) ionic liquid.

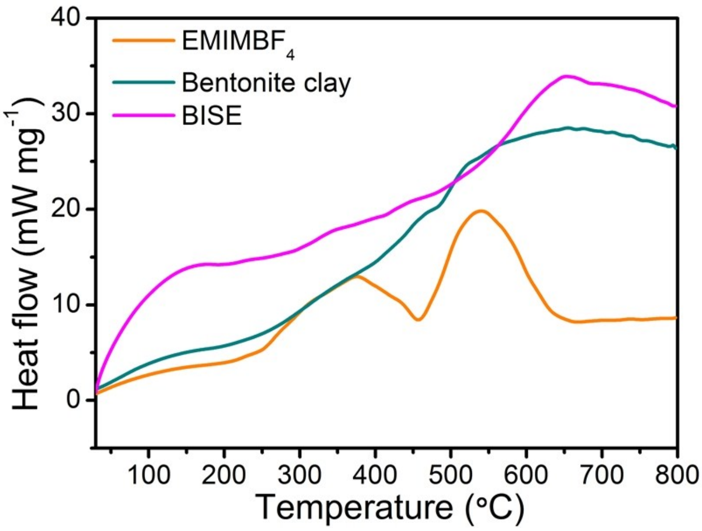

Fig. S5 The DSC curves of the $EMIMBF_4$, bentonite clay and the BISE. The weight loss of ionic liquid is mainly due to the volatilization of trace impurities and the decomposition and carbonization of ionic liquid. The weight loss of bentonite clay is mainly due to the evaporation of water adsorbed on the surface and between layers, and the decomposition of bentonite clay.

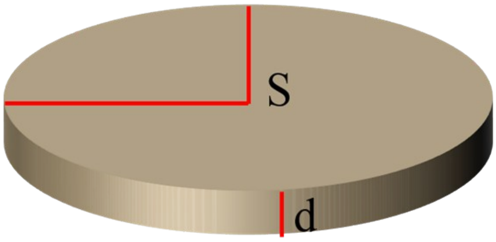

$$\sigma = \frac{d}{R \times S}$$

d (cm) — the thickness of the conductor;

R (Ω) — the conductor resistance;

S (cm^2) — the cross-sectional area of the conductor.

Fig. S6 The calculation of the ionic conductivity.

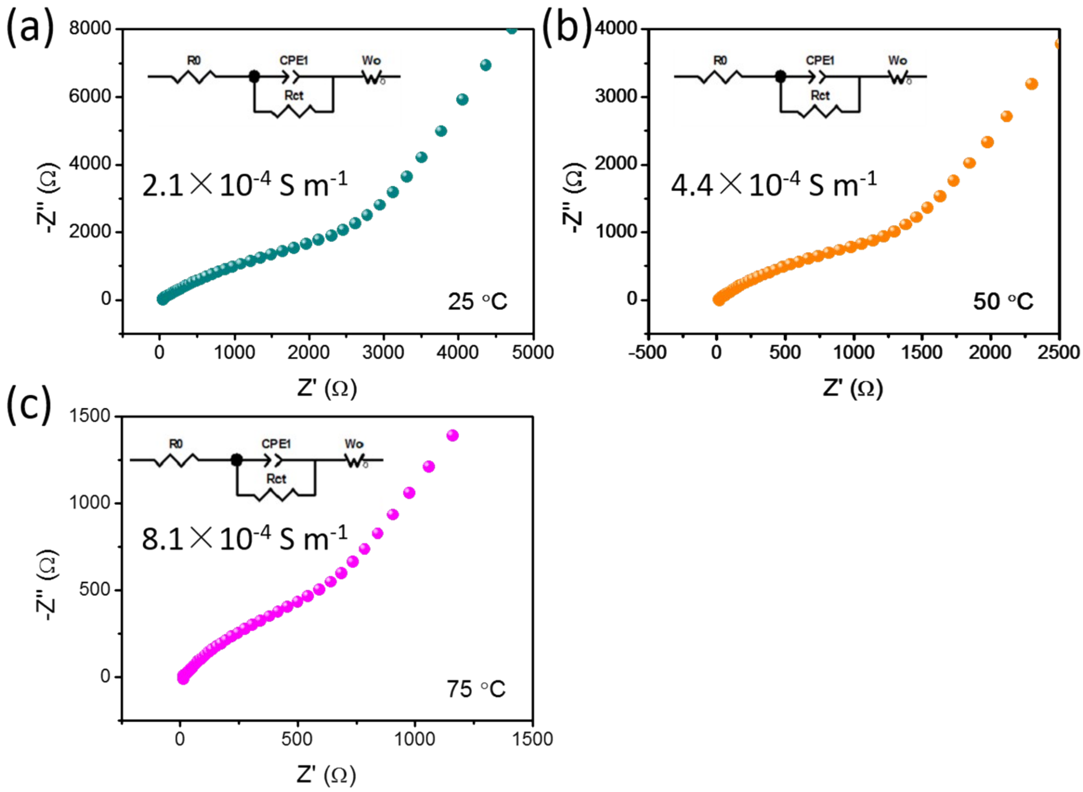

Fig. S7 EIS spectra of the BISE electrolyte at (a) 25 °C, (b) 50 °C and (c) 75 °C.

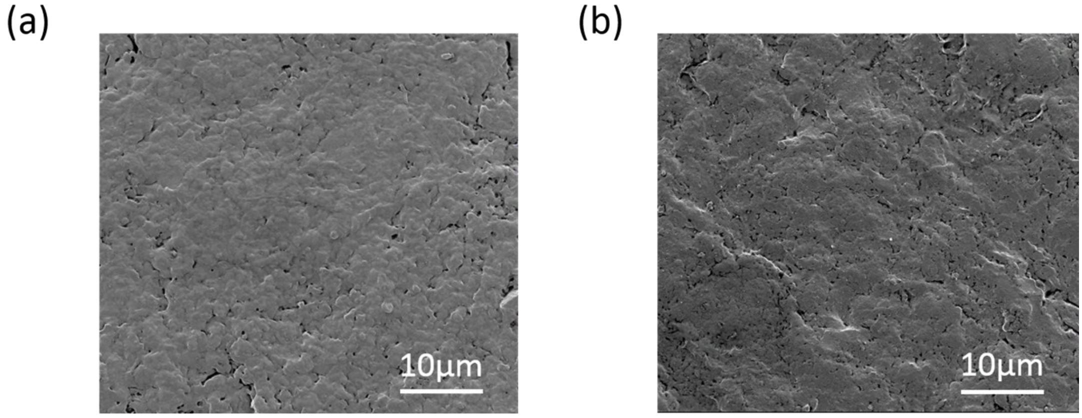

Fig. S8 SEM images of the BISE. (a) Before the self-discharge, (b) after the self-discharge.

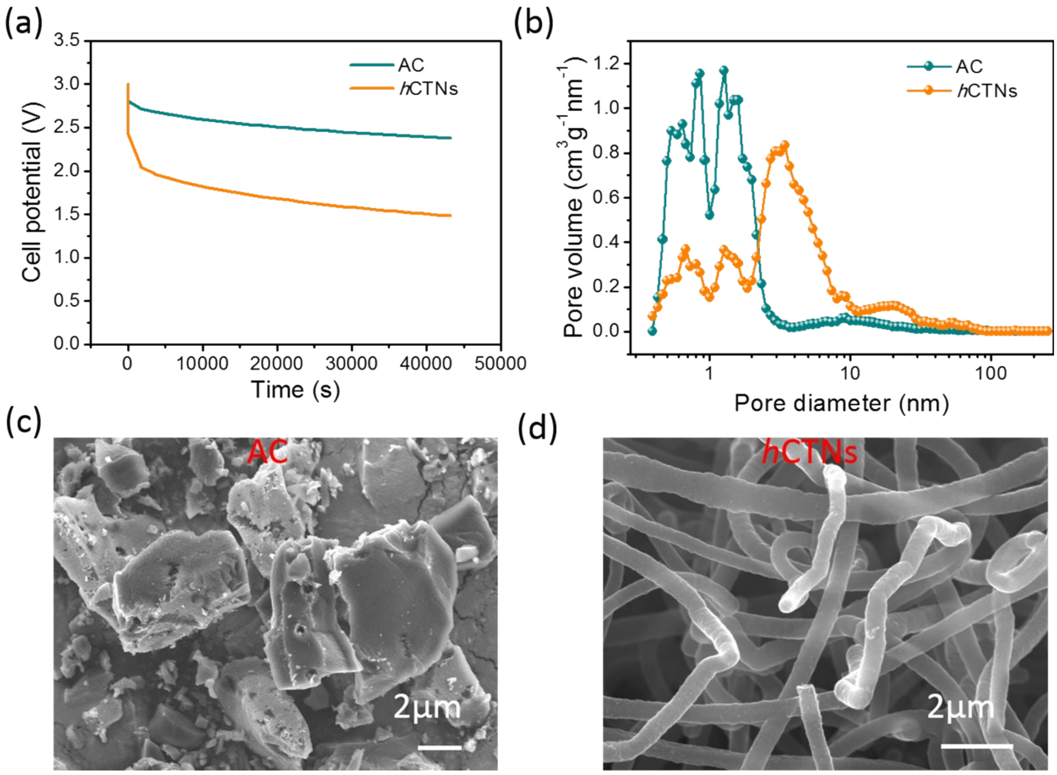

Fig. S9 The self-discharge of different electrode materials. **(a)** Decay of open circuit potential for the AC based supercapacitor and *h*CTNs based supercapacitor. **(b)** The corresponding pore size distributions of the AC and *h*CTNs calculated by density functional theory. SEM images of the **(c)** AC and **(d)** *h*CTNs.

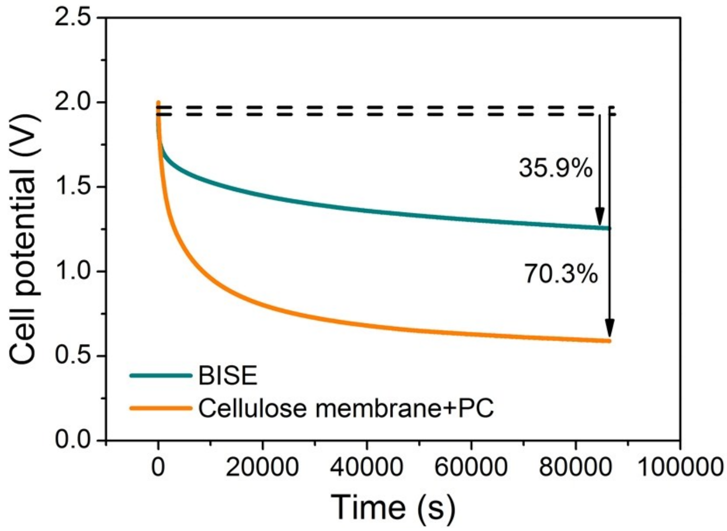

Fig. S10 Open circuit potential decays for conventional supercapacitors and BISE solid-state supercapacitors. BISE-based supercapacitors show a very low self-discharge rate of only 35.9% after 24 h. In contrast, the open circuit potential of the conventional supercapacitors with cellulose membrane dropped by 70.3%. Therefore, this BISE can not only reduce the self-discharge of supercapacitors with ionic liquid electrolyte, but also reduce the self-discharge of supercapacitors with commercial organic electrolyte.

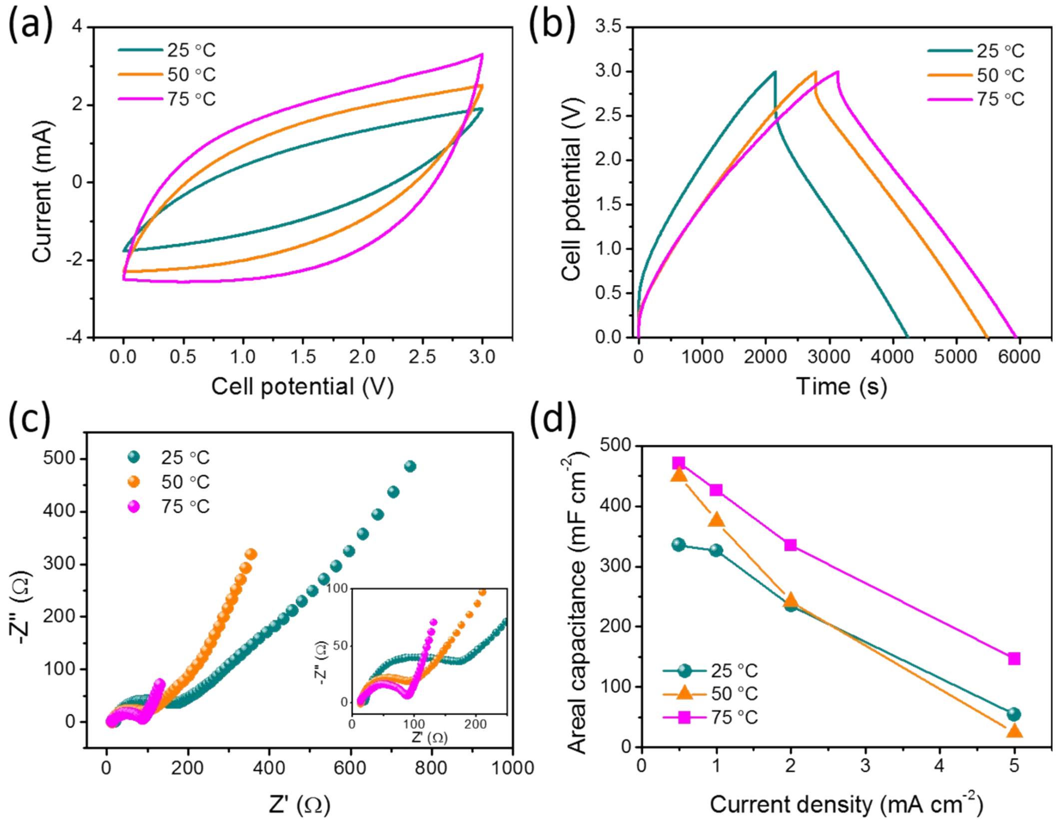

Fig. S11 Electrochemical properties of BISE-based supercapacitors in different temperatures. (a) Typical CV curves of BISE-based supercapacitors in different temperatures at a scan rate of 5 mV s^{-1}. **(b)** GCD curves of BISE-based supercapacitors in different temperatures at a current density of 0.5 mA cm^{-2}. **(c)** Nyquist plots. **(d)** The areal capacitance values at different current densities.

Supplementary Table

Table. S1 The comparison of BISE-based supercapacitors with most other reported supercapacittors.

Electrode	Electrolyte	Approach used	Self-discharge rate	Refs
AC	0.5M biredox IL in BMImTFSI IL	biredox ionic liquids	2.8→2.5 V (6 h 11%)	[1]
AC	6 M KOH	surfactant additives	0.8→0.504 V (20 h 37%)	[2]
AC	$PYR_{14}TFSI$	ionic liquids	2.8→1.5 V (72 h 46%)	[3]
N-doped carbon nanosheets	0.5 M H_2SO_4	o-benzenediol functional group grafted carbon electrodes	1.4→0.7 V (4 h 50%)	[4]
AC	1 M $TEMABF_4$ in acetonitrile	nematic liquid crystal 5CB as an additive in electrolyte	2.0→1.42 V (24 h 29%)	[5]
ACF	$TEABF_4$/PC	tailoring the electrode/electrolyte configuration	2.0→1.2 V (48 h 40 %)	[6]
SWNT macrofilms	1 M $TEABF_4$/PC	surface chemistry modification of electrodes	2.0→0.5 V (14.92 h 75%)	[7]
AC	PSiP/IL solid electrolyte	PSiP/IL solid electrolyte	2.5→1.5 V (48 h 60 °C 40%)	[8]
N-doped porous graphene	$EMIMBF_4$	graphene electrode prepared from moltensalt method	3.0→1.5 V (4.3 h 50%)	[9]
AC	1 M tetrabutylammonium hexafluorophosphate	ultra-thin insulating block layer	2→1.44 V (1 h 28%)	[10]
YP-80F	$BMImBF_4$	ionic liquids	2.5→1.44 V (24 h 42%)	[11]
Graphene hydrogel	1 M H_2SO_4	Nafion membrane as the separator	0.8→0.3 V (3.2 h 63%)	[12]
AC	$SnF_2/VOSO_4/H_2SO_4$ aqueous electrolyte	an ion exchange membrane	1.4→1.2 V (10 h 14%)	[13]
AC	Na_2SO_4/ Potassium Ferricyanide aqueous electrolyte	cation exchange membrane	0.8→0.6 V (10 h 25%)	[14]
AC fiber cloth	Potassium poly(acrylate) and KOH aqueous solution	polymer hydrogel electrolyte	0.8→0.2 V (40 h 75%)	[15]
AC	Bentonite clay@ionic liquid based solid-state electrolyte	confinement effect of ion transfer	3.0→2.0 V (60 h 29%)	This work

Reference

[1] Mourad, Eléonore, Coustan L, Lannelongue P, et al. Biredox ionic liquids with solid-like redox density in the liquid state for high-energy supercapacitors. Nature Materials, 2017, 16(4):446-453.

[2] Fic K, Lota G, Frackowiak E. Electrochemical properties of supercapacitors operating in aqueous electrolyte with surfactants. Electrochimica Acta, 2010, 55(25):7484-7488.

[3] Francesca S, Catia A, Marina M. Leakage currents and self-discharge of ionic liquid-based supercapacitors. Journal of Applied Electrochemistry, 2014, 44(4):491-496.

[4] Ting X, Zhi Y, Wee L, et al. o-benzenediol Functionalized Carbon Nanosheets as Low Self-Discharge Aqueous Supercapacitor. ChemSusChem, 2018, 11, 3307.

[5] Xia M, Nie J, Zhang Z, et al. Suppressing Self-Discharge of Supercapacitors via Electrorheological Effect of Liquid Crystals. Nano Energy, 2018, 47.

[6] Zhang Q, Rong J, Ma D, et al. The governing self-discharge processes in activated carbon fabric-based supercapacitors with different organic electrolytes. Energy & Environmental Science, 2011, 4.

[7] Zhang Q, Cai C, Qin J, et al. Tunable self-discharge process of carbon nanotube based supercapacitors. Nano Energy, 2014, 4(1):14-22.

[8] Sato T, Marukane S, Morinaga T, et al. High voltage electric double layer capacitor using a novel solid-state polymer electrolyte. Journal of Power Sources, 2015, 295:108-116.

[9] Wang J, Ding B, Hao X, et al. A modified molten-salt method to prepare graphene electrode with high capacitance and low self-discharge rate. Carbon, 2016, 102:255-261.

[10] Tevi T, Yaghoubi H, Wang J, et al. Application of poly (p-phenylene oxide) as blocking layer to reduce self-discharge in supercapacitors. Journal of Power Sources, 2013, 241(Complete):589-596.

[11] Laheäär, Ann, Ana A D L P, Béguin. François. Change of self-discharge

mechanism as a fast tool for estimating long-term stability of ionic liquid based supercapacitors. Journal of Power Sources, 2018, 396:220-229.

[12] Libin Chen, Hua Bai, Zhifeng Huang, et al. Mechanism investigation and suppression of self-discharge in active electrolyte enhanced supercapacitors. Energy & Environmental Science, 7.

[13] Juhan L, aAura T, Benjamin K, et al. Asymmetric tin–vanadium redox electrolyte for hybrid energy storage with nanoporous carbon electrodes. Sustainable Energy & Fuels, 2017, 1:299-307.

[14] Lee J, Choudhury S, Weingarth D, et al. High performance hybrid energy storage with potassium ferricyanide redox electrolyte. Acs Applied Materials & Interfaces, 1944, 8(36):23676.

[15] Nohara S, Wada H, Furukawa N, et al. Self-discharge characteristics of an electric double-layer capacitor with polymer hydrogel electrolyte. Research on Chemical Intermediates, 2006, 32(5):491-496.